Strasbourg (France)

MANUSCRIPT COVER PAGE FORM

E-MRS Symposium : D

Paper number : #20??

Title of paper : BIMODAL DISTRIBUTION OF DAMAGE MORPHOLOGY GENERATED BY ION IMPLANTATION

Corresponding author : K. R. C. Mok

Full Mailing Address : Caroline Mok. Dpto. Electronica. Universidad de Valladolid. E.T.S.I.T. Campus Miguel Delibes S/N. 47011. Valladolid. Spain.

Telephone : +34 983 42 30 00 ext 5510

Fax : +34 983 42 36 75

E-mail : g0202446@nus.edu.sg

Bimodal distribution of damage morphology generated by ion implantation

K. R. C. Mok,[1,2] M. Jaraiz,[1] I. Martin-Bragado,[1,3] J. E. Rubio,[1]
P. Castrillo,[1] R. Pinacho,[1] M. P. Srinivasan,[2] and F. Benistant[4]

[1]*Departamento de E. y Electrónica,*
Universidad de Valladolid. ETSIT Campus Miguel Delibes, 47011 Valladolid, Spain
[2]*Department of Chemical & Biomolecular Engineering,*
National University of Singapore. 4 Engineering Drive 4, Singapore 117576
[3]*Synopsys. Karl-Hammerschmidt Strasse 34,*
D-85609 Aschheim/Dornach, Germany
[4]*Chartered Semiconductor Manufacturing. 60 Woodlands*
Industrial Park D, Street 2, Singapore 738406.

Abstract

A nucleation and evolution model of damage based on amorphous pockets (APs) has recently been developed and implemented in an atomistic kinetic Monte Carlo simulator. In the model, APs are disordered structures (I_nV_m), which are agglomerates of interstitials (I) and vacancies (V). This model has been used to study the composition and size distribution of APs during different ion implantations. Depending strongly on the dose rate, ion mass and implant temperature, the APs can evolve to a defect population where the agglomerates have a similar number of I and V (n≈m), or to a defect population with pure I (m≈0) and pure V (n≈0) clusters, or a mixture of APs and clusters. This behavior corresponds to a bimodal (APs/clusters) distribution of damage. As the AP have different thermal stability compared to the I and V clusters, the same damage concentration obtained through different implant conditions has a different damage morphology and, consequently, exhibit a different resistance to subsequent thermal treatments.

I. INTRODUCTION

Extensive experimental and theoretical studies have been done on ion-implantation induced damage. A complex and wide diversity of damage types have been revealed by various studies. For example, single cascades in silicon studied by molecular dynamics (MD) [1] result in the production of amorphous pockets (APs) (a mixture of interstitials (I) and vacancies (V)), as well as isolated point defects and small pure I and V clusters. The thermal stability of these different defect types has been studied both theoretically and experimentally, and found to be very different. Pure I [2] and V [3] clusters are more thermally stable than APs or amorphous regions, with higher activation energy for cluster emission than the activation energy for recrystallization [4–6].

A nucleation and evolution model of damage based on damage structures known as the APs has been developed and it is able to reproduce many experimentally observed features of damage accumulation, like the damage dependence on ion mass, implant temperature and dose rate. Using the model as an analysis tool, it reveals a bimodal (APs/pure clusters) distribution of damage. Therefore it can be used to predict not only the damage level but also its morphology obtained from different implant conditions. As the different damage types have different thermal annealing behaviour, this has implications of practical relevance for silicon processing.

II. OUR MODEL

The damage accumulation model used in this work is based on the damage structures known as APs [1] and has been implemented in a kinetic Monte Carlo simulator [7]. I and V are assumed to form an AP when they are within a capture distance (second neighbor distance) of each other. An AP is therefore an agglomerate of I's and V's surrounded by crystalline silicon. Here, the I and V terms are used as a means of referring (for an $\mathrm{I}_n\mathrm{V}_m$ AP) to a disordered region of a volume size roughly equal to $n\mathrm{I}+m\mathrm{V}$ with a net excess or deficit of atoms n-m. In this model, pure interstitials ($\mathrm{I}_n\mathrm{V}_0$) and vacancy clusters ($\mathrm{I}_0\mathrm{V}_m$) are considered to be subsets of the APs, with their own characteristic emission rates [2, 3]. Once an AP with a net excess of I's or V's has completely recrystallized, for example during dynamic annealing, the remaining I's or V's behave as pure clusters. Similarly, as the implant

proceeds, with new collision cascades, pure clusters can transform back into an I_nV_m AP and have a chance of recrystallizing if a defect of the opposite type is within its capture radius. This allows for a self-consistent treatment of pure clusters and APs (I_nV_m).

In this approach, the AP recrystallization rate (shrinkage rate) is characterized by the effective size of the AP (s=min(n, m)). An AP of size s is assumed to shrink to $(s-1)$ at a rate given by $\alpha s^{\beta} \exp(-E_{\text{act}}(s)/kT)$ with the activation energy for recrystallization as a function of s alone, irrespective of the internal spatial configuration. This model has been able to reproduce the amorphous-crystalline transition temperature from experimental data [8], as a function of dose rate, for (100) silicon irradiated with 80 keV ions to a dose of $1 \times 10^{15}\,\text{cm}^{-2}$ for Si and Ge, and $2 \times 10^{15}\,\text{cm}^{-2}$ for C.

Figure 1 shows 2D histograms of the APs of varying compositions (I_nV_m) and clusters (n=0 or m=0) for an 80 keV, $2\times10^{15}\,\text{cm}^{-2}$ C implant at the amorphous-crystalline transition temperature (20°C at a dose rate of $5\times10^{12}\,\text{cm}^{-2}\text{s}^{-1}$). The color represents the concentration of I's and V's in APs of a given composition (I, V axes). Initially (Fig. 1(a)), the APs are generally well balanced in I and V composition, showing a trend towards a small deficit of atoms (nI<mV), in agreement with MD observations [9]. Figure 1(b) clearly shows the split of the defect population into the bimodal distribution of damage. As the implant proceeds, the amount of small APs decreases until there are no APs smaller than a certain size s. The smaller APs have recrystallized and the net excess of I or V in these APs behave now as pure I and V clusters (pixels adjacent to the axes). Only larger APs that are stable at the given implant temperature remain. The same behaviour is observed for heavier ions, only extended to larger sizes. To attain the amorphous-crystalline transition with a heavier ion, the same amount of damage has to be accumulated. However, since heavier ion generates more damage and it is extended to larger APs sizes, damage (small APs) has to be removed up to larger sizes, which also results in more pure clusters. This implies that different implant conditions can lead to different substrate morphology. This model therefore provides a useful analysis tool that could give an insight into the damage morphology resulting from different implant conditions, and the consequences in the face of subsequent thermal treatments.

III. SIMULATION RESULTS

A constant damage concentration of $1\times10^{21}\,\mathrm{cm}^{-3}$ was obtained from 80 keV Si implant at a constant dose rate of $5\times10^{12}\,\mathrm{cm}^{-2}\mathrm{s}^{-1}$ using different combinations of dose and temperature. The different damage morphology after each implant is shown in Fig. 2. Damage morphology in terms of APs with a well balanced distribution of I, V can be obtained with a low temperature implant. At some intermediate temperature, a bimodal distribution with a mixture of pure clusters and amorphous pockets is obtained. At high implant temperature, damage accumulates as pure I or V clusters only.

The different initial damage morphologies at the same damage concentration were then used as a starting point for subsequent annealing at 800 °C. Figure 3 shows the different annealing behaviour. The damage induced by room temperature implant, anneal out very quickly compared to the more stable damage induced by the 200 °C implant. During the annealing of the damage induced by the room temperature implant, the sharp drop in damage in the first 3 s, corresponds to the recrystallization of APs. Figure 4 shows a snapshot of the AP distribution during this time. In the next 10 s, decrease in damage comes from the emission of I, V clusters. Subsequently, only I clusters, including some {311} defects are left to be annealed. In the case of annealing of the damage induced by the 200 °C implant, the initial slower drop in damage is due to I, V cluster emission. Then damage remains constant predominantly due to stable {311} defects, though V clusters are also present.

IV. CONCLUSIONS

We have shown that at the same damage level, different implant conditions can lead to different damage morphology, consisting of APs, pure clusters or a mixture of both. Since APs and clusters have different thermal stability, with clusters being more stable and hence more difficult to anneal, the same amount of damage with different morphology, consequently leads to different annealing behavior with interesting practical implications.

List of References

---

[1] M. J. Caturla, T. Diaz de la Rubia, L. A. Marques, and G. H. Gilmer, Phys. Rev. B **54**, 16683 (1996).

[2] N. E. B. Cowern, G. Mannino, P. A. Stolk, F. Roozeboom, H. G. A. Huizing, J. G. M. van Berkum, F. Cristiano, A. Claverie, and M. Jaraiz, Phys. Rev. Lett. **82**, 4460 (1999).

[3] A. Bongiorno, L. Colombo, and T. Diaz de la Rubia, Europhys. Lett. **43**, 695 (1998).

[4] L. A. Marques, L. Pelaz, M. Aboy, L. Enriquez, and J. Barbolla, Phys. Rev. Lett. **91**, 135504 (2003).

[5] S. E. Donnelly, R. C. Birtcher, V. M. Vishnyakov, and G. Carter, Appl. Phys. Lett. **82**, 1860 (2003).

[6] K. A. Jackson, J. Mater. Res. **3**, 1218 (1988).

[7] M. Jaraiz, P. Castrillo, R. Pinacho, I. Martin-Bragado, and J. Barbolla, in *Simulation of Semiconductor Processes and Devices 2001*, edited by D. Tsoukalas and C. Tsamis (Springer-Verlag, Vienna, 2001), pp. 10–17.

[8] R. D. Goldberg, J. S. Williams, and R. G. Elliman, Nucl. Instrum. Meth. B **106**, 242 (1995).

[9] K. Nordlund, M. Ghaly, R. S. Averback, M. Caturla, T. Diaz de la Rubia, and J. Tarus, Phys. Rev. B **57**, 7556 (1998).

List of figure captions

FIG 1. 2D histogram of AP composition of amorphizing Carbon implant at (a) 10% and (b) 80% of the total dose

FIG 2. 2D histogram of AP composition showing the damage composition at a constant damage level of $1 \times 10^{21}\,\mathrm{cm}^{-3}$, resulting from 80 keV Si implant at dose rate of $5 \times 10^{12}\,\mathrm{cm}^{-2}\mathrm{s}^{-1}$. (a) Implant temperature of -100 °C and a dose of $2 \times 10^{13}\,\mathrm{cm}^{-2}$ (b) Implant at room temperature and a dose of $5 \times 10^{13}\,\mathrm{cm}^{-2}$ (c) Implant at 200°C and a dose of $1 \times 10^{15}\,\mathrm{cm}^{-2}$.

FIG 3. Annealing behaviour of damage induced by room temperature implant and by 200 °C implant at 800 °C.

FIG 4. A snapshot of AP composition during annealing of the damage induced by room temperature implant.

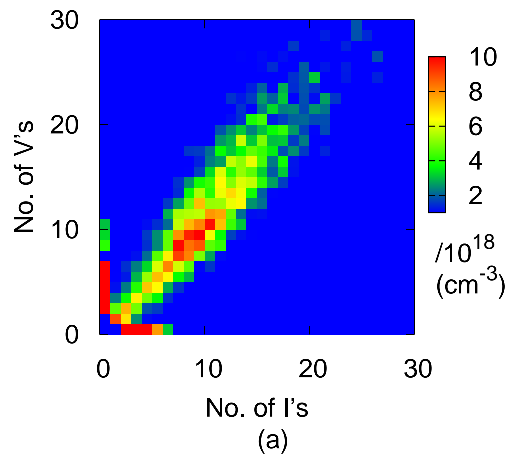

(a)

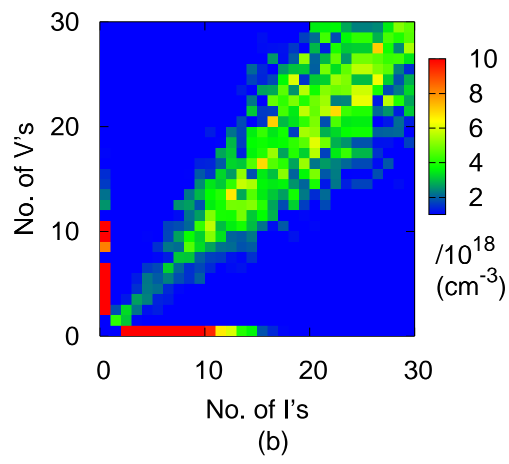

(b)

FIG. 1:

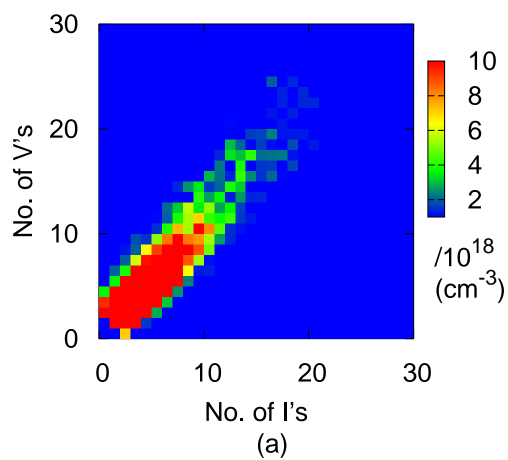

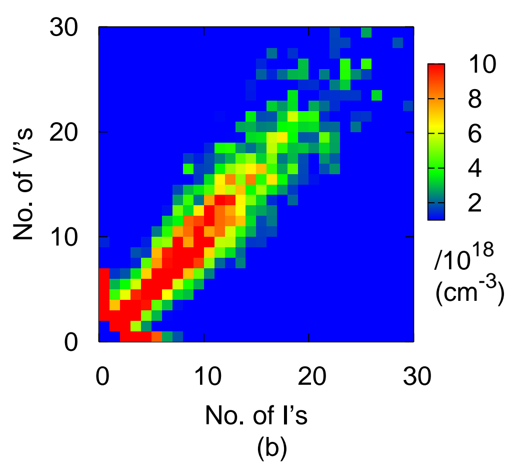

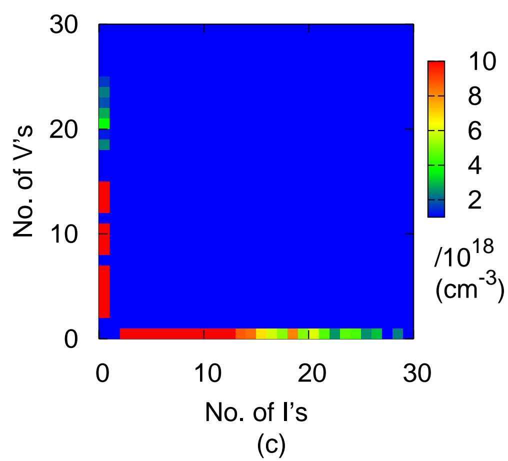

FIG. 2:

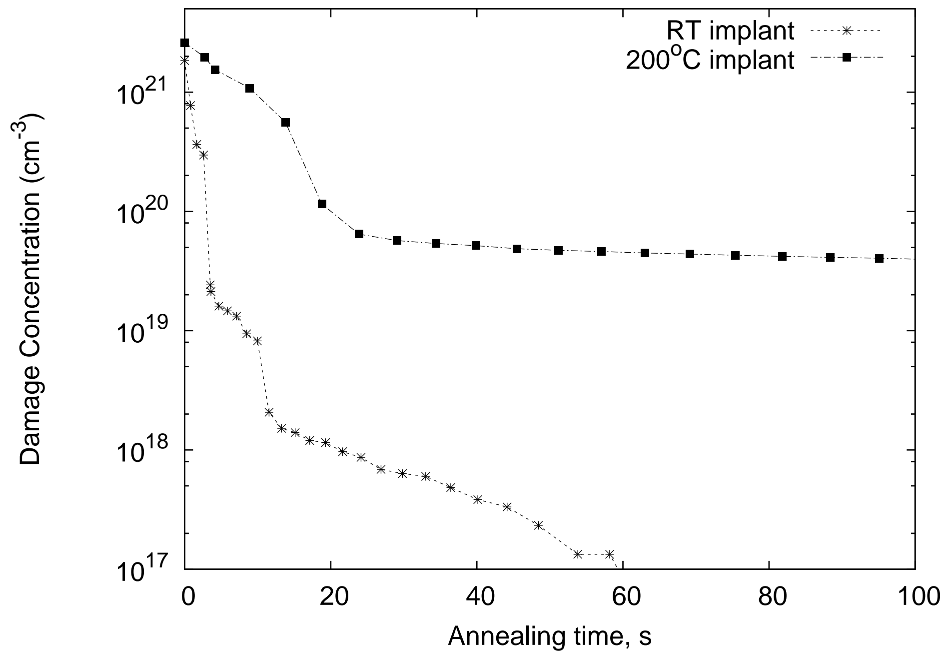

FIG. 3:

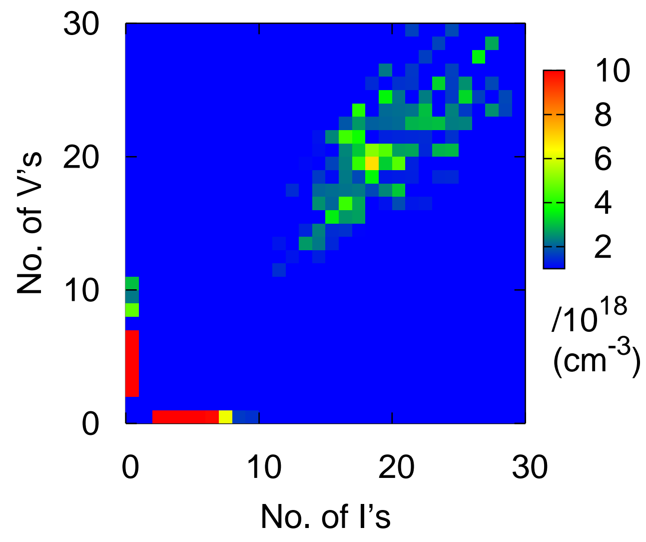

FIG. 4: